CUT&RUN reveals unique positioning of pre-initiated RNA polymerase II in the steady state of transcription

Michi Miura[#] and Honglin Chen

State Key Laboratory for Emerging Infectious Diseases and

Department of Microbiology, The University of Hong Kong,

Hong Kong SAR, China

[#]Email: michi.miura.res@gmail.com

Abstract

CUT&RUN is a powerful tool to study protein-DNA interactions *in vivo*. DNA fragments cleaved by the targeted micrococcal nuclease identify the footprints of DNA-binding proteins on the chromatin. We applied a variant of the current CUT&RUN protocol to human lung carcinoma cell line A549 in a 24-well cell culture plate to profile RNA polymerase II. Long (>270 bp) DNA fragments corresponded to the bimodal peak around the transcription start sites, as previously seen with chromatin immunoprecipitation. However, we found that shorter (<120 bp) fragments identify a well-defined peak localised at the transcription start sites. This distinct DNA footprint indicates the unique positioning of the poised RNA polymerase II before transcription initiation, which has not been detected in the steady state of transcription by standard chromatin immunoprecipitation. We propose that this method, which we call "CUT&RUN on plate", is an efficient way of investigating protein-DNA interactions in adherent cells in culture.

Keywords: CUT&RUN; protein-DNA interaction; RNA polymerase II; transcription initiation; promoter-proximal pausing; chromatin profiling

38 # Introduction

39 CUT&RUN (Cleavage Under Targets and Release Using Nuclease) (Skene & Henikoff,
40 2017) is a powerful tool to map protein-DNA interactions *in vivo*. CUT&RUN directs
41 Protein A/G-fused micrococcal nuclease (pAG-MNase) (Meers, Bryson, Henikoff, &
42 Henikoff, 2019) to the antibody-bound protein-DNA complex, with a subsequent release
43 of the DNA fragments cleaved in the presence of calcium ions. There are two major
44 advantages of CUT&RUN over conventional chromatin immunoprecipitation (ChIP).
45 First, CUT&RUN does not require sonication for chromatin fragmentation. Physical
46 shearing of chromatin by sonication does not occur randomly, which can skew signal
47 detection; and excessive sonication may attenuate the epitope of the target protein
48 (Marx, 2019). Second, CUT&RUN identifies the footprints of DNA-binding proteins on
49 the chromatin, which revealed distinct binding configurations of transcription factors in
50 yeast (Skene & Henikoff, 2017) and mammalian cells (Meers, Janssens, & Henikoff,
51 2019).

52 The current CUT&RUN protocol (Hainer & Fazzio, 2019; Meers, Bryson, et al., 2019;
53 Skene, Henikoff, & Henikoff, 2018) relies on Concanavalin A-coated magnetic beads to
54 immobilise the cells before the targeted pAG-MNase cleavage. This immobilisation step
55 introduces a range of shortcomings associated with the use of Concanavalin A-beads.
56 For example, trypsinisation while harvesting the cells may alter the behaviour of DNA-
57 binding proteins and lower the binding affinity of cells to Concanavalin A. Concanavalin
58 A also stimulates certain types of cells and alters the behaviour of DNA-binding proteins.
59 When the plasma membrane is removed to investigate the nuclei, Concanavalin A does
60 not bind efficiently to the nuclear membrane. Finally, Concanavalin A-beads tend to
61 aggregate when cells are attached.

62 To circumvent the use of Concanavalin A-beads, we devised a variant of the CUT&RUN
63 protocol to streamline the conventional procedure for adherent cells on a multi-well cell
64 culture plate (Figure 1A). Since the entire protocol is carried out on a single plate, we
65 dub our methodology "CUT&RUN on plate" or CROP. This method was applied to the
66 human lung carcinoma cell line A549 to profile RNA polymerase II (Pol II) around the
67 transcription start sites (TSS). We found that CROP could validate the bimodal signal
68 around the TSS as previously detected using ChIP (Erickson, Sheridan, Cortazar, &
69 Bentley, 2018). However, we also identified a distinct peak at the TSS from short DNA
70 fragments released only by pAG-MNase. This finding indicates a transient positioning
71 of the pre-initiated RNA polymerase II in the steady state of transcription, which has
72 eluded detection by conventional ChIP (Erickson et al., 2018).

73

74 # Results

75 **Overall performance of "CUT&RUN on plate" for profiling Pol II**

76 We tested the feasibility of the CROP protocol with Pol II antibodies on the adherent
77 human lung carcinoma cell line A549. Pol II signals obtained by CROP are shown in
78 Figure 1B. The genomic region chr6 p22.2 was selected due to the presence of multiple
79 histone genes. This location is ideal for efficient visual inspection of Pol II signals
80 because of the compact size and close spacing of these genes. Our Pol II signals
81 consistently mapped to the transcription units of histone genes with low background as
82 previously reported (Meers, Bryson, et al., 2019; Skene & Henikoff, 2017) (Figure 1B).
83 The signals along the gene body, in addition to 1.5 kb upstream of the TSS and
84 downstream of the transcription end site (TES), were averaged over "singletons" (genes
85 that are separated from other genes by >2 kb) (Figure 1C), showing consistent

86 enrichment around the TSS. Therefore, through the successful capture of Pol II signals
87 *in situ* with low background, the performance of our CROP protocol was shown to be
88 comparable with the conventional CUT&RUN (Meers, Bryson, et al., 2019; Skene &
89 Henikoff, 2017).

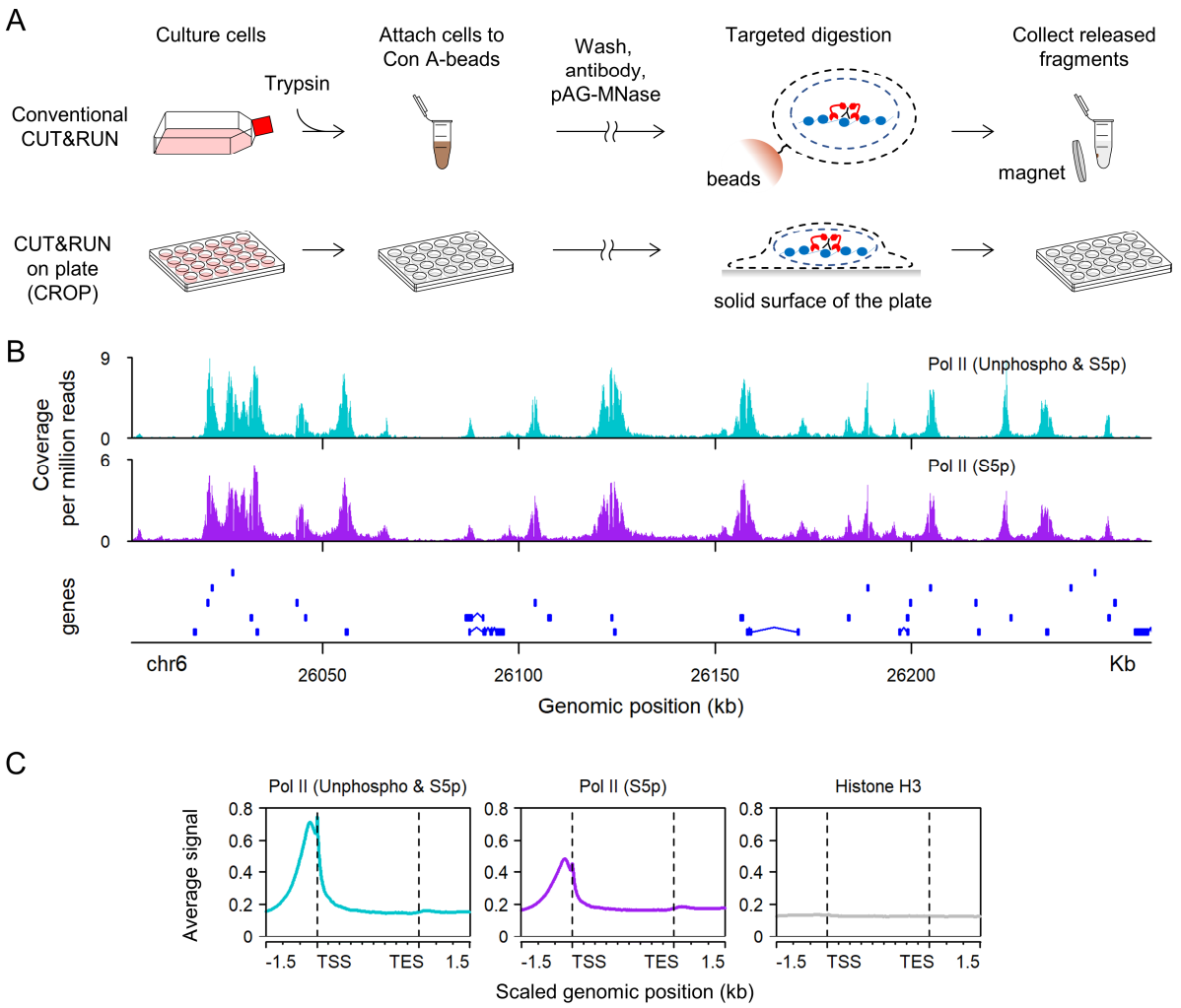

90

91 **Figure 1 Overall performance of "CUT&RUN on plate"**

92 (A) Protocol overview. In conventional CUT&RUN (top row), cells are harvested and attached on
93 Concanavalin A-magnetic beads. Subsequent cell permeabilisation, antibody binding, and targeted pAG-
94 MNase digestion are performed on these cells immobilised on the beads. The magnetic beads are captured
95 each time the buffers are changed. "CUT&RUN on plate" (or CROP) (bottom row) circumvents the use of
96 Concanavalin A-magnetic beads. Adherent cells are anchored on the solid surface of the multi-well plate
97 throughout the protocol, enabling rapid buffer change for multiple samples. (B) Pol II signals in the histone

gene cluster obtained by CROP. The Pol II signal is expressed by the coverage normalised with the total read count. (C) Metaplot analysis of the Pol II signal. Pol II signal was averaged over genes that are at least 2 kb away from other genes. The region between 1.5 kb upstream of the transcription start site (TSS) and 1.5 kb downstream of the transcription end site (TES) is presented. The length of the gene body is scaled to 3 kb.

Size-fractionation of aligned reads to reveal distinct footprints of Pol II-binding

The size distribution of aligned paired-end reads showed multiple peaks (Figure 2A). We categorised the aligned reads into 5 subsets by length (Figure 2A), each of which is expected to reflect a unique footprint of the protein-DNA interaction (Meers, Janssens, et al., 2019; Skene & Henikoff, 2017). The size of DNA fractions was shown to reveal distinct signals of Pol II around the TSS (Figure 2B). The signal of the total reads (i.e. without size-fractionation) conformed to the characteristic bimodal peak as previously reported by ChIP (i.e. the peaks located at either ~150 bp upstream or downstream of the TSS) (Erickson et al., 2018). By contrast, the shorter fragments (<120 bp) constituted a single narrow peak at the TSS, and the longer fragments (>120 bp) accumulated adjacent to the TSS (Figure 2B). As expected, the bimodal signal of the longer fragments (>270 bp) is skewed towards the region downstream of the TSS (Figure 2B) (Erickson et al., 2018). To validate our findings, we analysed the TSS of individual genes. We confirmed that some genes showed an accumulation of longer (>270 bp) fragments on both sides of the TSS (Figure 2C), whereas some other genes had signals on only one side (Figure 2D and E). The signals of the shorter (<120 bp) and longer (>270 bp) fragments were mutually exclusive, showing two distinct footprints of Pol II adjacent to each other.

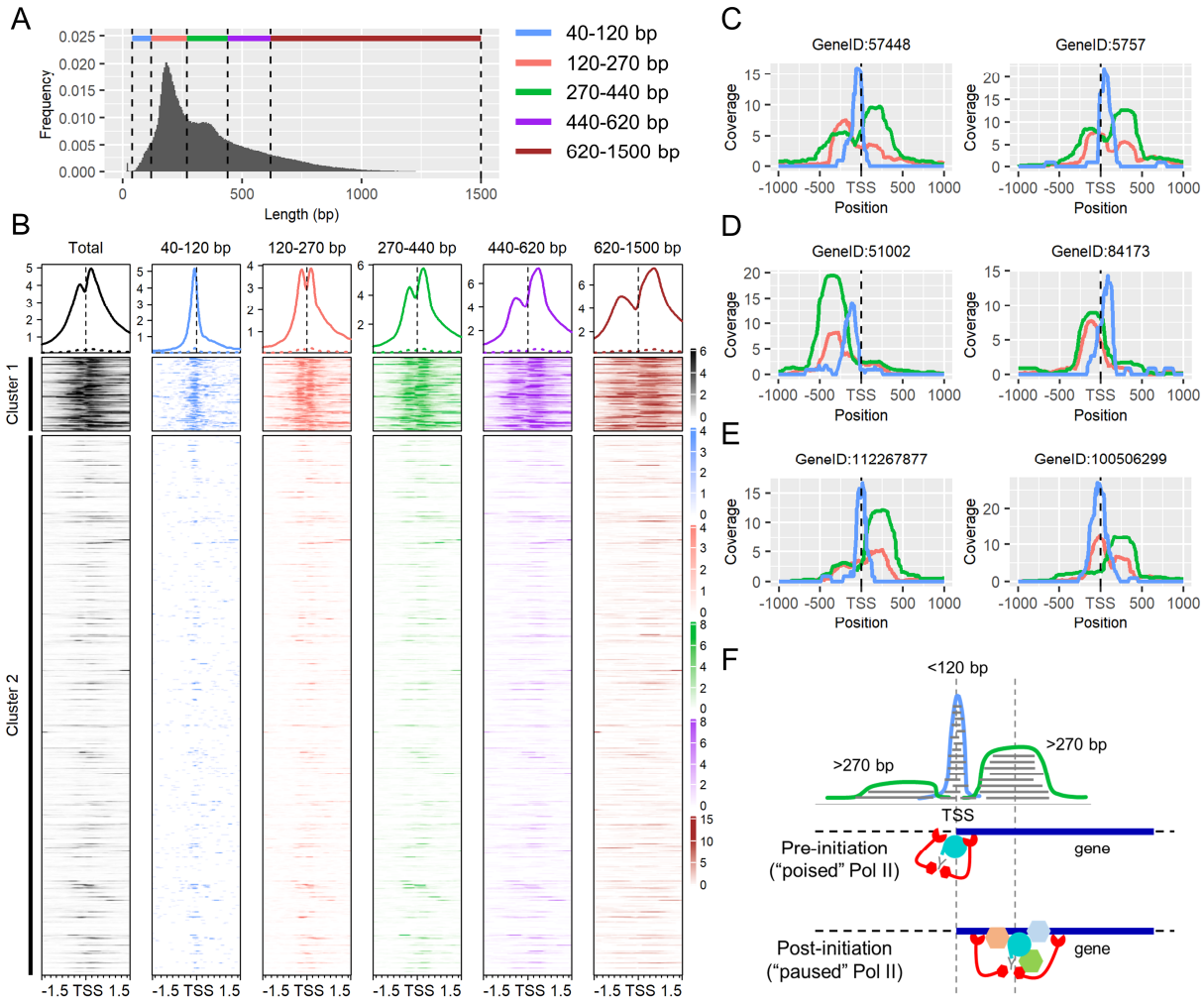

Figure 2 Size-fractionation identifies distinct Pol II footprints

(A) Size distribution of aligned reads (the insert size between the sequence adaptors). The reads were categorised into five subsets by size, each of which is coded by a unique colour. (B) Pol II signal (Millipore, 05-623; unphosphorylated and S5p) of each fraction of reads in ±1.5 kb around the transcription start site (TSS). The signals in 13,452 annotated RefSeq singleton genes are presented in the heatmap; a *k*-mean clustering was performed on the total reads (coded in black) to enrich genes with Pol II signal (Cluster 1 and Cluster 2). The metaplot for each cluster is shown above the heatmap (Cluster 1, solid line; Cluster 2, dashed line). (C-E) Pol II signal (Millipore, 05-623; unphosphorylated and S5p) in ±1 kb around the transcription start site of individual genes. The vertical axis indicates the pile-up of aligned reads from the three size fractions. The same colour codes are used as per panel (A). Note that the coverage was normalised per million reads within each of the size fractions; the relative coverage within each plot is not proportional to the actual frequency of these fractions. (F) A schematic drawing of the Pol II footprints deduced by the alignment of size-fractionated reads.

137 Recent studies using ChIP-seq, as well as nascent transcript sequencing, have shown
138 that Pol II is paused at ~50 bp downstream of the TSS (Core, Waterfall, & Lis, 2008;
139 Erickson et al., 2018; Kwak, Fuda, Core, & Lis, 2013; Nojima et al., 2015; Shao &
140 Zeitlinger, 2017). Our observations suggest two distinct binding configurations of Pol II
141 near the TSS (Figure 2F). These configurations are: (1) poised Pol II at the TSS in the
142 pre-initiation state where nucleosomes and other factors are depleted, and (2) paused
143 Pol II upstream or downstream of the TSS where Pol II pausing is regulated by a higher-
144 molecular complex after transcription initiation. The paused Pol II peaks were visible
145 exclusively in the longer (>120 bp) fragments adjacent to the TSS. We reason that this
146 is because Pol II is associated with a high-molecular complex at the paused site (Vos et
147 al., 2018), which protects the chromatin from the pAG-MNase cleavage. As a result,
148 pAG-MNase is unable to produce shorter (<120 bp) fragments associated with the
149 paused Pol II. Composite signals were observed in our assay (Figure 2C to E), each of
150 which corresponds to one of the two distinct binding configurations as described. These
151 composite signals result from CUT&RUN taking a 'snapshot' of each gene from hundreds
152 of thousands of cells per assay at the TSS; a transcription start site accommodates one
153 molecule of Pol II at a time, either at the TSS (pre-initiation) or the site of promoter-
154 proximal pausing (post-initiation) (Shao & Zeitlinger, 2017).

155

156 **Impact of formaldehyde fixation on "CUT&RUN on plate"**

157 Formaldehyde fixation is often used to investigate transient protein interactions. We
158 tested if formaldehyde fixation can be implemented in "CUT&RUN on plate". Cells were
159 fixed with 1.5% formaldehyde in either pre- or post-cellular permeabilisation (see
160 Materials and Methods). Although formaldehyde fixation reduced the detection of Pol II

161 signals, serine 5-phosphorylated (S5p) Pol II was shown to be enriched near the TSS

162 (Figure 3A).

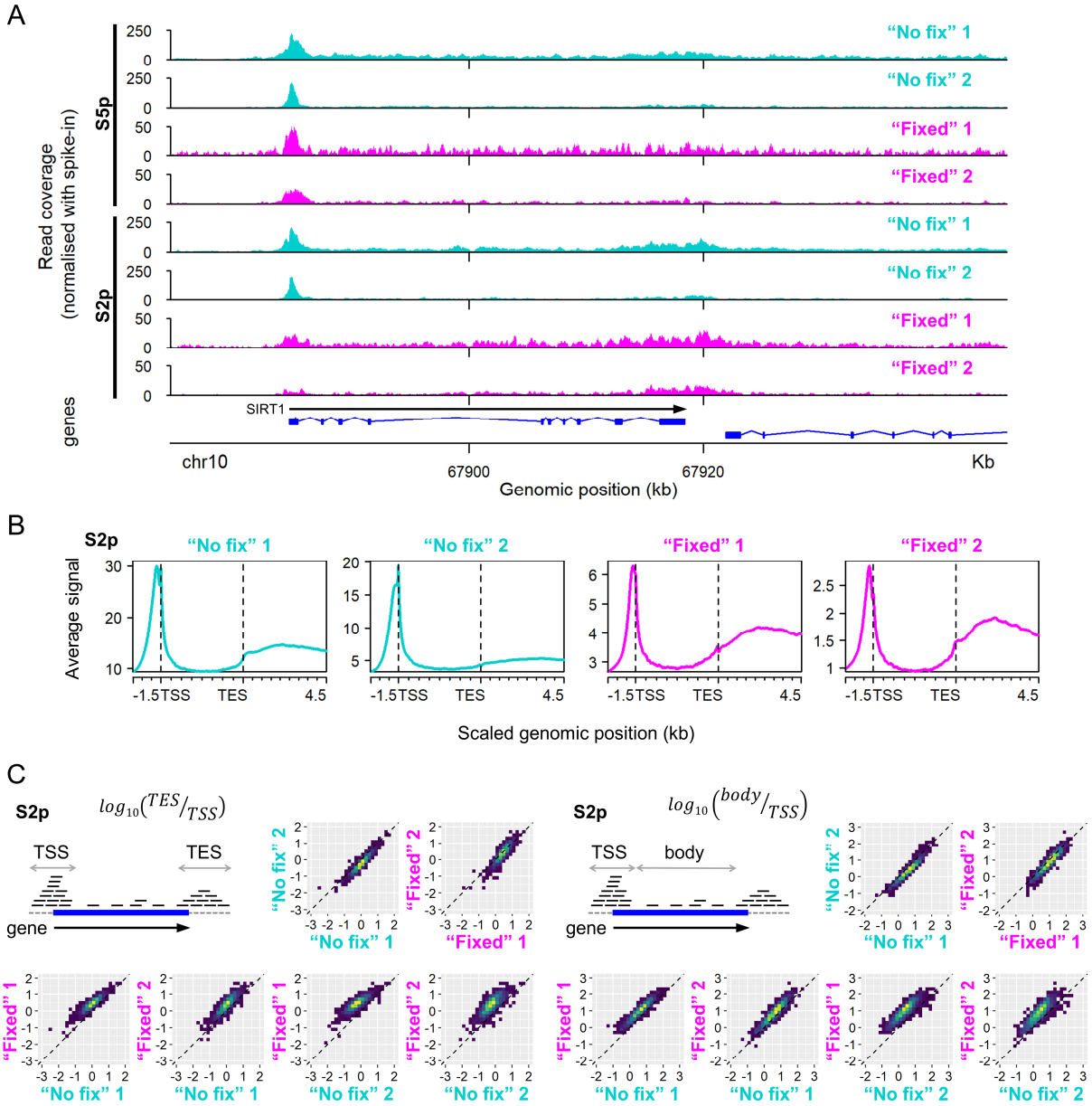

163

164 **Figure 3 Impact of formaldehyde cell fixation on the S2p Pol II signals**

165 (A) S5p and S2p Pol II signal coverage over a gene on chr10 (SIRT1) (S5p, ab5131; S2p, ab5095). Two colour
166 codes indicate whether cells were fixed with formaldehyde (cyan, "No fix"; magenta, "Fixed"). When
167 formaldehyde was used, cells were fixed following permeabilisation ("Fixed" 1) or fixed ahead of time
168 ("Fixed" 2). The signals were normalised with the yeast spike-in DNA. (B) Metaplot analyses of S2p Pol II

signal from 1.5 kb upstream of the transcription start site (TSS) to 4.5 kb downstream of the transcription end site (TES). The signals were averaged over the singleton genes (n = 13,452). The gene body is scaled to 4.5 kb in length. (C) Two Pol II metrics measuring the ratio of signals in the gene body to TSS (left) and in the TES to TSS (right). These metrics were calculated for genes (n = 1,435) that were longer than 5 kb and aggregated in Cluster 1 (Figure 2B). The metrics of each gene are plotted for each combination of the assays and the density of plots are represented by colour brightness (navy to yellow). The data is presented in the logarithmic scale (base = 10) for ease of visualisation.

We observed a profound effect of formaldehyde fixation on the serine 2-phosphorylated (S2p) Pol II signal (Figure 3A). The metaplot analysis showed that the average signal of S2p RNA polymerase II over the singleton genes was more pronounced in the region downstream of the TES when cells were fixed (Figure 3B). This observation was confirmed by signal quantification in the gene body or TES (relative to that in the TSS respectively), for each singleton gene (Figure 3C, schematic drawing). While these metrics for each gene were in good concordance within the same fixation condition, we found that the ratio of S2p Pol II signal in the gene body to TSS, or in the TES to TSS was higher when the cells were fixed (Figure 3C, “No Fix” vs “Fixed”). We consider two possible explanations of this observation: (1) fixation stabilises the elongating S2p RNA polymerase II on the DNA, and (2) fixation preferentially reduces the detection of Pol II near the TSS, thereby altering the ratio of signals in the TSS, gene body and TES.

Discussion

The turnover of Pol II near the TSS is highly dynamic (Darzacq et al., 2007; Erickson et al., 2018; Steurer et al., 2018). Since the duration of Pol II in the promoter-proximal pausing state is about ten times longer than that of Pol II in the pre-initiation state (Darzacq et al., 2007; Steurer et al., 2018), a majority of reads obtained by either ChIP

195 or CUT&RUN is captured from the paused site, approximately 50 bp downstream of the
196 TSS. Because ChIP fragments are typically hundreds of base pairs long, the rare signal
197 of the poised Pol II at the TSS is often obscured. While Erickson *et al.* had previously
198 identified the signal of the poised Pol II at the TSS by ChIP, this signal was only exposed
199 following the depletion of Pol II in hypotonic condition with the use of triptolide to block
200 the initiation (Erickson et al., 2018). In contrast, we accurately identified the positioning
201 of poised Pol II in the steady state of transcription through the recovery of its unique
202 footprint (Figure 2F).

203 In this study, we have devised "CUT&RUN on plate" (CROP) for profiling protein-DNA
204 interactions in adherent cells. By using 24-well cell culture plates, a batch of an assay
205 can accommodate up to 24 unique combinations of experimental conditions and
206 antibodies targeting the proteins of interest. We anticipate that CROP can be
207 downscaled into a 96-well plate that would accommodate tens of thousands of adherent
208 cells, which is sufficient for a typical CUT&RUN assay to detect histone modifications
209 (Skene et al., 2018; Skene & Henikoff, 2017). This would make it possible to design a
210 high-throughput CROP assay in combination with an automated liquid dispenser.

211 In conclusion, CUT&RUN is an effective substitute for the conventional chromatin
212 immunoprecipitation (Skene & Henikoff, 2017), yet not many laboratories have adapted
213 the technique due to the complexity associated with the use of Concanavalin A-beads.
214 The protocol described here overcomes certain key problems in the existing CUT&RUN
215 technique, and may find widespread application.

216 # Materials and Methods

217 **Cells**

218 Human lung carcinoma cell line A549 was maintained in Dulbecco's Modified Eagle
219 Medium (Gibco, 11965-092) supplemented with 10% FBS (Gibco, 16140-071), 100 U/ml
220 penicillin and 100 μg/ml streptomycin (Gibco, 15140-122).

221

222 **CUT&RUN in a cell culture plate**

223 CUT&RUN was performed on a standard 24-well cell culture plate (TPP, 92012); cells
224 were left attached to the bottom of the well throughout the protocol.

225 A549 was seeded in wells and grown to ~70 to 90% confluency (~0.5 million cells) at the
226 time of an assay. Cells were washed with PBS and permeabilised with Perm buffer (0.1%
227 Triton X-100 (Sigma, X100), 20 mM HEPES-KOH pH 7.5, 150 mM NaCl, 0.5 mM
228 Spermidine (Sigma, S2626) and proteinase inhibitor (Roche, 04 693 132 001)) for 15
229 min at room temperature. After removing Perm buffer, cells were washed again with
230 Perm buffer and incubated with an antibody (~0.7 μg) in 150 μl Perm buffer per well for
231 one hour at room temperature. The antibodies used in this study were: mouse anti-
232 RNA polymerase II (Millipore, 05-623; clone CTD4H8; 0.75 μg per well); rabbit anti-RNA
233 polymerase II (phospho S2) (Abcam, ab5095; polyclonal; 0.75 μg per well); and rabbit
234 anti-RNA polymerase II (phospho S5) (Abcam, ab5131; polyclonal; 0.675 μg per well).
235 After incubation, unbound antibody was removed, and cells were washed twice with
236 Perm buffer. Cells were then incubated with the recombinant pAG-MNase (Cell
237 Signaling, 40366; 1:33 volume) in 150 μl Perm buffer per well for an hour at room
238 temperature. Unbound pAG-MNase was removed, and cells were washed twice with

239 Perm buffer. During the second wash of this stage, the plate was placed on ice-cold
240 water. For pAG-MNase activation, 150 µl ice-cold Perm buffer containing 5 mM $CaCl_2$
241 was dispensed per well, and the plate was incubated on ice-cold water for 30 min. The
242 pAG-MNase digestion was halted by the addition of 50 µl 4× STOP solution (680 mM
243 NaCl, 40 mM EDTA (Sigma, E5134), 8mM EGTA (AG Scientific, E-2491), 100 µg/ml
244 RNase A (Invitrogen, 12091021) and 0.1% Triton X-100). The plate was incubated at
245 37°C for 30 min to facilitate the release of digested DNA fragments from the nucleus.
246 The supernatant was collected, and DNA was extracted using DNeasy Blood & Tissue
247 Kit (Qiagen, 69504).

248 In addition to the native "CUT&RUN on plate" described above, two protocols for cell
249 fixation with 1.5% formaldehyde were tested: (1) cells were fixed with 1.5% formaldehyde
250 for 10 min prior to the cell permeabilisation with Perm buffer; and (2) cells were fixed
251 following the permeabilisation (5 min in Perm buffer). The supernatant collected at the
252 end of the CUT&RUN protocol was supplemented with 1% SDS (final concentration) and
253 incubated at 65°C overnight for de-crosslinking. The DNA was purified with QIAquick
254 PCR Purification Kit (Qiagen, 28104).

255

256 **Pair-end sequencing and read alignment**

257 DNA libraries were constructed using NEBNext Ultra II DNA Library Prep Kit for Illumina
258 (NEB, E7645) with index primers (NEB, E7335 and E7710). Fragmented genomic DNA
259 from *S. cerevisiae* (Cell Signaling, 40366) was used (10 pg per sample) as spike-in.

260 DNA libraries were sequenced (150 bp × 2) with NovaSeq 6000 (Illumina), and the initial
261 50 bases of each read were aligned to a concatenation of human reference genome
262 (GRCh38) and *S. cerevisiae* (sacCer3) with a BWA algorithm (version 0.7.17) `bwa mem`

263 (Li & Durbin, 2009). Duplications of reads were marked with a Picard tool (version
264 2.18.9) `MarkDuplicates` (http://broadinstitute.github.io/picard). Only a minority of
265 the aligned reads (less than 0.151%) constituted the yeast genome, thereby confirming
266 the successful recovery of DNA fragments cleaved by pAG-MNase. A subset of aligned
267 reads was selected for the downstream analyses using Samtools (version 1.9) with the
268 following commands: SAM flag 3 (read paired; read mapped in proper pair) (`samtools
269 view -f 3`); mapping quality greater than 20 (`samtools view -q 20`); without tags
270 `'XA:Z:'` and `'SA:Z:'` (`grep -v -e 'XA:Z:' -e 'SA:Z:'`); and aligned in either one of
271 the chromosomes chr1 to chr22, chrX or chrY (`samtools view chr1 chr2 ... chrY`).

272

273 **Data analyses and visualisation**

274 Aligned reads were fractionated by size (the 9th field of SAM) and stored in the BAM
275 format. Read coverage was computed and stored in the bigWig format with deepTools's
276 (version 3.1.3) `bamCoverage` (Ramirez et al., 2016), normalised per million reads. For
277 comparison of the Pol II signals across the fixation conditions (Figure 3A and B), read
278 coverage was computed with deepTools's (version 3.3.2) `bamCoverage` using scale
279 factors calculated with the number of spike-in reads mapped to the yeast genome. The
280 bigWig files were converted into the bedGraph format using `bigWigToBedGraph` (UCSC)
281 and the read coverage was visualised with the R package Sushi (version 1.24.0)
282 (Phanstiel, Boyle, Araya, & Snyder, 2014) in R (version 3.6.2). A matrix containing the
283 read coverage over a given region of genes was computed using deepTools's (version
284 3.3.2) `computeMatrix` with an annotation
285 GCA_000001405.15_GRCh38_full_analysis_set.refseq_annotation (NCBI). A subset of
286 genes that were separated from other genes by >2 kb was considered for this analysis;

287 such genes were extracted using bedtools's (version 2.26.0) (Quinlan & Hall, 2010)
288 `merge` and `intersect`. The matrix was visualised as a heatmap and a metaplot using
289 the R package EnrichedHeatmap (version 1.16.0) (Gu, Eils, Schlesner, & Ishaque, 2018).

290

291 **Signal quantification in the TSS, gene body and TES**

292 The regions for TSS, gene body and TES were defined: TSS, ±0.5 kb around the start
293 site of a gene; gene body, from 0.5 kb downstream of the start site to 1.5 kb upstream
294 of the end site; and TES, 1.5 kb upstream of the end site to 4.5 kb downstream of the
295 end site. For each of the TSS, gene body and TES regions, genome coordinates for the
296 singleton genes in the RefSeq annotation were stored in the BED format.

297 The BAM files containing the aligned paired reads were converted into the BED format
298 with bedtools's `bamtobed -bedpe` and the subsequent extraction of the 1st
299 (chromosome), 2nd, 6th (the start and end positions of an alignment, respectively), 7th,
300 8th and 9th fields.

301 For each singleton gene, paired reads aligned to the TSS, gene body or TES were counted
302 using bedtools's `intersect -F 0.5` (reads that overlapped by less than half of the
303 alignment length were rejected). The read counts in the gene body and TES were
304 normalised with the number of reads contained in the TSS.

Acknowledgements

We thank Liew Jun Mun at University of Cambridge, for reviewing the manuscript to enhance the readability. We also thank Prof. Charles R. M. Bangham at Imperial College London, for reviewing the manuscript and critical comments. Illumina NovaSeq 6000 sequencing was performed at Centre for PanorOmic Sciences (CPOS) Genomics Core, LKS Faculty of Medicine, The University of Hong Kong. This study was supported in part by the Research Grants Council of the Hong Kong SAR (17119618, 17107019 and C7027-16G).

Competing interests

The authors declare no competing interests.

316 **References**

317 Core, L. J., Waterfall, J. J., & Lis, J. T. (2008). Nascent RNA sequencing reveals
318 widespread pausing and divergent initiation at human promoters. *Science,*
319 *322*(5909), 1845-1848. doi:10.1126/science.1162228

320 Darzacq, X., Shav-Tal, Y., de Turris, V., Brody, Y., Shenoy, S. M., Phair, R. D., & Singer,
321 R. H. (2007). In vivo dynamics of RNA polymerase II transcription. *Nat Struct Mol*
322 *Biol, 14*(9), 796-806. doi:10.1038/nsmb1280

323 Erickson, B., Sheridan, R. M., Cortazar, M., & Bentley, D. L. (2018). Dynamic turnover
324 of paused Pol II complexes at human promoters. *Genes Dev, 32*(17-18), 1215-
325 1225. doi:10.1101/gad.316810.118

326 Gu, Z., Eils, R., Schlesner, M., & Ishaque, N. (2018). EnrichedHeatmap: an
327 R/Bioconductor package for comprehensive visualization of genomic signal
328 associations. *BMC Genomics, 19*(1), 234. doi:10.1186/s12864-018-4625-x

329 Hainer, S. J., & Fazzio, T. G. (2019). High-Resolution Chromatin Profiling Using
330 CUT&RUN. *Curr Protoc Mol Biol, 126*(1), e85. doi:10.1002/cpmb.85

331 Kwak, H., Fuda, N. J., Core, L. J., & Lis, J. T. (2013). Precise maps of RNA polymerase
332 reveal how promoters direct initiation and pausing. *Science, 339*(6122), 950-953.
333 doi:10.1126/science.1229386

334 Li, H., & Durbin, R. (2009). Fast and accurate short read alignment with Burrows-
335 Wheeler transform. *Bioinformatics, 25*(14), 1754-1760.
336 doi:10.1093/bioinformatics/btp324

337 Marx, V. (2019). What to do about those immunoprecipitation blues. *Nat Methods, 16*(4),
338 289-292. doi:10.1038/s41592-019-0365-3

339 Meers, M. P., Bryson, T. D., Henikoff, J. G., & Henikoff, S. (2019). Improved CUT&RUN
340 chromatin profiling tools. *Elife, 8*. doi:10.7554/eLife.46314

341 Meers, M. P., Janssens, D. H., & Henikoff, S. (2019). Pioneer Factor-Nucleosome Binding
342 Events during Differentiation Are Motif Encoded. *Mol Cell, 75*(3), 562-575 e565.
343 doi:10.1016/j.molcel.2019.05.025
344 Nojima, T., Gomes, T., Grosso, A. R. F., Kimura, H., Dye, M. J., Dhir, S., . . . Proudfoot,
345 N. J. (2015). Mammalian NET-Seq Reveals Genome-wide Nascent Transcription
346 Coupled to RNA Processing. *Cell, 161*(3), 526-540.
347 doi:10.1016/j.cell.2015.03.027
348 Phanstiel, D. H., Boyle, A. P., Araya, C. L., & Snyder, M. P. (2014). Sushi.R: flexible,
349 quantitative and integrative genomic visualizations for publication-quality multi-
350 panel figures. *Bioinformatics, 30*(19), 2808-2810.
351 doi:10.1093/bioinformatics/btu379
352 Quinlan, A. R., & Hall, I. M. (2010). BEDTools: a flexible suite of utilities for comparing
353 genomic features. *Bioinformatics, 26*(6), 841-842.
354 doi:10.1093/bioinformatics/btq033
355 Ramirez, F., Ryan, D. P., Gruning, B., Bhardwaj, V., Kilpert, F., Richter, A. S., . . .
356 Manke, T. (2016). deepTools2: a next generation web server for deep-sequencing
357 data analysis. *Nucleic Acids Res, 44*(W1), W160-165. doi:10.1093/nar/gkw257
358 Shao, W., & Zeitlinger, J. (2017). Paused RNA polymerase II inhibits new transcriptional
359 initiation. *Nat Genet, 49*(7), 1045-1051. doi:10.1038/ng.3867
360 Skene, P. J., Henikoff, J. G., & Henikoff, S. (2018). Targeted in situ genome-wide
361 profiling with high efficiency for low cell numbers. *Nat Protoc, 13*(5), 1006-1019.
362 doi:10.1038/nprot.2018.015
363 Skene, P. J., & Henikoff, S. (2017). An efficient targeted nuclease strategy for high-
364 resolution mapping of DNA binding sites. *Elife, 6*. doi:10.7554/eLife.21856

365 Steurer, B., Janssens, R. C., Geverts, B., Geijer, M. E., Wienholz, F., Theil, A. F., . . .
366 Marteijn, J. A. (2018). Live-cell analysis of endogenous GFP-RPB1 uncovers rapid
367 turnover of initiating and promoter-paused RNA Polymerase II. *Proc Natl Acad Sci*
368 *U S A, 115*(19), E4368-E4376. doi:10.1073/pnas.1717920115
369 Vos, S. M., Farnung, L., Boehning, M., Wigge, C., Linden, A., Urlaub, H., & Cramer, P.
370 (2018). Structure of activated transcription complex Pol II-DSIF-PAF-SPT6.
371 *Nature, 560*(7720), 607-612. doi:10.1038/s41586-018-0440-4

372